

Anomalous supercurrent modulated by interfacial magnetizations in Josephson junctions with ferromagnetic bilayers


Hao Meng^{1,2,3}, Xiuqiang Wu⁴, Yajie Ren,² and Jiansheng Wu^{1,3,*}

¹*Shenzhen Institute for Quantum Science and Engineering (SIQSE), Southern University of Science and Technology, Shenzhen 518055, China*

²*School of Physics and Telecommunication Engineering, Shaanxi University of Technology, Hanzhong 723001, China*

³*International Quantum Academy, Shenzhen, 518048, China*

⁴*Department of Physics, Yancheng Institute of Technology, Yancheng 224051, China*

 (Received 15 April 2022; revised 16 October 2022; accepted 18 October 2022; published 1 November 2022)

Based on the Bogoliubov–de Gennes equations, we investigate the transport of the Josephson current in a $S/f_L\text{-}F_1\text{-}f_C\text{-}F_2\text{-}f_R/S$ junction, where S and $F_{1,2}$ are superconductors and ferromagnets, and $f_{L,C,R}$ are the left, central, and right spin-active interfaces. These interfaces have noncollinear magnetizations, and the azimuthal angles of the magnetizations at the $f_{L,C,R}$ interfaces are $\chi_{L,C,R}$. We demonstrate that, if both the ferromagnets have antiparallel magnetizations, the critical current oscillates as a function of the exchange field and the thickness of the ferromagnets for particular χ_L or χ_R . By contrast, when the magnetization at the f_C interface is perpendicular to that at the f_L and f_R interfaces, the critical current reaches a larger value and is hardly affected by the exchange field and the thickness. Interestingly, if both the ferromagnets are converted to antiparallel half-metals, the critical current maintains a constant value and rarely changes with the ferromagnetic thicknesses and the azimuthal angles. At this time, an anomalous supercurrent can appear in the system, in which case the Josephson current still exists even if the superconducting phase difference ϕ is zero. This supercurrent satisfies the current-phase relation $I = I_c \sin(\phi + \phi_0)$ with I_c being the critical current and $\phi_0 = 2\chi_C - \chi_L - \chi_R$. We deduce that the additional phase ϕ_0 arises from phase superposition, where the phase is captured by the spin-triplet pairs when they pass through each spin-active interface. In addition, when both the ferromagnets are transformed into parallel half-metals, the f_C interface never contributes any phase to the supercurrent and $\phi_0 = \chi_R - \chi_L + \pi$. In such a case, the current-phase relation is similar to that in a $S/f_L\text{-}F\text{-}f_R/S$ junction.

DOI: [10.1103/PhysRevB.106.174502](https://doi.org/10.1103/PhysRevB.106.174502)

I. INTRODUCTION

In recent years great attention was paid to the study of superconductor (S)/ferromagnet (F) heterostructures due to plenty of fascinating phenomena that have been predicted and observed [1–7]. It is well known that ferromagnetism and spin-singlet superconductivity are two inimical orders, as ferromagnetism favors a parallel spin alignment, while spin-singlet Cooper pairs consist of electrons with antiparallel aligned spins. Consequently, the ferromagnetic exchange field will make a dephasing effect on the electrons of the spin-singlet pairs [2,3], when a F is adjacent to a conventional s -wave S. In hybrid S/F structures with homogeneous magnetization, the spin-singlet pairs ($\uparrow\downarrow - \downarrow\uparrow$) are destroyed by the exchange field of the F layer, so that they penetrate the F layer over a rather short scale. Meanwhile, the spin-triplet pairs ($\uparrow\downarrow + \downarrow\uparrow$) generate at the S/F interface and rapidly decay in the F layer. In contrast, the magnetic inhomogeneities could mediate equal-spin triplet pairs where both electrons are in the same spin band—either the majority band for spin-up triplet pairs ($\uparrow\uparrow$) or the minority band for spin-down triplet pairs ($\downarrow\downarrow$). Such triplet pairs are immune to the exchange field and can therefore penetrate the ferromagnet over a long distance

from the S/F interface that the spin-singlet pairs could not reach [2–7].

In a uniform ferromagnetic Josephson junction (S/F/S), the wave function of the Cooper pairs penetrates ferromagnet on a short distance of the order $\xi_F = \hbar v_f/2h$ for ballistic systems and $\xi_F = \sqrt{\hbar D}/h$ for diffusive ones, where v_f is the Fermi velocity, h is ferromagnetic exchange field, and D is the electronic diffusion constant [2]. Meanwhile, this penetration is accompanied by oscillations of the wave function in space. As a result, the critical current will reverse sign with changing temperature and thickness of the F layer (see [2] and references cited therein). Besides, in the Josephson junction with a nonuniform exchange field, the long-range supercurrent is apparent because the equal-spin triplet pairs ($\uparrow\uparrow$) [or ($\downarrow\downarrow$)] occur in the F layer [3–6]. The penetration depth of these triplet pairs into a ferromagnet is much longer than ξ_F and may be of the order of the Cooper pair penetration length into a normal metal, $\xi_N = \hbar v_f/2\pi T$ for ballistic systems and $\xi_N = \sqrt{\hbar D}/2\pi T$ for diffusive ones, where T is the temperature [2].

On the other hand, in a traditional ferromagnetic Josephson junction, the ground state energy usually switches between specific superconducting phase differences $\phi = 0$ and π , and the current-phase relation is sinusoidal $I(\phi) = I_c \sin \phi$, with I_c being the critical current flowing through the junction [1]. In the presence of breaking chiral [8] and time-reversal symmetry [1] in the Cooper pairs tunneling process, a spon-

*wuj@sustech.edu.cn

taneous supercurrent at zero phase difference can arise, and the Josephson ground state can be characterized by a superconducting phase difference ϕ_0 . This supercurrent satisfies the current-phase relation $I(\phi) = I_c \sin(\phi + \phi_0)$ [1]. This ϕ_0 junction could introduce excellent opportunities to quantum computer bits. It has been reported that the ϕ_0 junction can be realized in Josephson junctions with ferromagnetic interlayers or under an externally applied Zeeman field in the presence of spin-orbit coupling [8–21], as well as with inhomogeneous ferromagnetic interlayers without an external spin-orbit coupling [22–33].

It was theoretically predicted several years ago that the long-range triplet pairs with equal spins could be induced by the inhomogeneous magnetization configuration in the Josephson junctions [34–46]. The prediction of the long-range penetration of the spin-triplet pairs into a ferromagnet was observed in multiple experiments [47–63]. It is very much worth noting that Houzet *et al.* [37] proposed an alternative Josephson junction geometry of the form $S/f_L\text{-F-}f_R/S$ in which the magnetization directions of the f_L and f_R layers are noncollinear to the central F layer. They suggested measuring the critical current in the Josephson junction to demonstrate the equal-spin triplet pairs. Soon after, the Birge group [52–54] observed a long-range supercurrent in Josephson junctions of the form $S/f_L\text{-Co-Ru-Co-}f_R/S$, where the central Co-Ru-Co trilayer was a synthetic antiferromagnet. The thin Ru layer induces antiparallel exchange coupling between the domains in the two Co layers, leaving nearly zero net magnetization in the junctions. To qualitatively explain the above experiments, the theoretical works of Volkov *et al.* [43] and Trifunovic *et al.* [44] utilizing the quasiclassical theory studied the spatial distribution of spin-singlet and spin-triplet pair amplitudes and the long-range spin-triplet Josephson current in the $S/f_L\text{-F}_1\text{-F}_2\text{-}f_R/S$ junction.

There are three questions to be solved urgently: (i) The experiments found that, without the Ru layer, the critical currents were very small [52–54]. However, in both theoretical works [43,44], the Ru layer was regarded as a nonmagnetic metal and thus its influence on the transport of the spin-triplet pairs was not considered. (ii) It is known that the majority spin-triplet component has a larger amplitude than the minority spin-triplet component in the strong ferromagnet. In the $S/f_L\text{-F}_1\text{-F}_2\text{-}f_R/S$ junction, when magnetizations of the F_1 and F_2 layers are antiparallel to each other, the majority spin-triplet pairs in the F_1 layer become minority spin-triplet pairs in the F_2 layer and vice versa. As a result, both triplet components suffer from the lower transmission amplitude of the minority component somewhere in the system. If that were the whole story, then the Josephson current should be small. In particular, the current is completely inhibited when the F_1 and F_2 layers are turned into antiparallel half-metals. This inference is inconsistent with the critical current enhancement observed in the experiments [52–54]. (iii) The quasiclassical approximation used by both theoretical works [43,44] does not consider the fact that the transport properties of the majority and minority electrons at the Fermi surface in the F_1 and F_2 layers are very different, in which case the spontaneous supercurrent cannot be captured.

The purpose of this paper is to address the three questions raised above. Recently, Quarterman *et al.* [64] experimentally

demonstrated that ferromagnetism can occur in ultrathin Ru films. This evidence can be used to address questions (i) and (ii) mentioned above. The Ru layer with noncollinear magnetizations can induce a spin-flip scattering effect, which converts the spin-up (spin-down) triplet pairs in the F_1 layer to the spin-down (spin-up) triplet pairs in the F_2 layer. In this process, the Ru layer acts as a bridge connecting the F_1 and F_2 layers to ensure supercurrent transmission. To address question (iii), we employ a microscopical approach to solve the Bogoliubov–de Gennes (BdG) equations [65]. The exact numerical solutions of these equations can acquire the spontaneous supercurrent.

In this paper we study the propagation of long-range Josephson current in the $S/f_L\text{-F}_1\text{-}f_C\text{-F}_2\text{-}f_R/S$ junction, where $F_{1,2}$ are antiparallel or parallel ferromagnets, and $f_{L,C,R}$ denote the left, central, and right spin-active interfaces. All these interfaces have noncollinear magnetizations, and the azimuthal angles of the magnetizations at the $f_{L,C,R}$ interfaces are $\chi_{L,C,R}$. When the F_1 and F_2 layers are antiparallel to each other, the Josephson critical current exhibits different characteristics for the different azimuthal angles of the interfaces. If the azimuthal angle χ_L or χ_R takes particular values, the critical current will oscillate with increasing exchange field and thickness of the F_1 and F_2 layers. For other values of χ_L or χ_R , the oscillation effect of the current hardly appears. By comparison, when the magnetization of the f_C interface is perpendicular to that of the f_L and f_R interfaces, the critical current reaches a higher value and is essentially unaffected by the exchange field and thickness.

Interestingly, when both ferromagnetic layers turn into antiparallel half-metals, in which case the very large magnetization strength permits only one spin to exist, the critical current always remains a constant value and is rarely affected by the ferromagnetic thicknesses and the azimuth angles. At this time, the Josephson current gains an additional phase $\phi_0 = 2\chi_C - \chi_L - \chi_R$ to form the spontaneous supercurrent. We consider that the phase ϕ_0 arises from the phase superposition effect, where the phase is obtained by the spin-triplet pairs when they transport through each spin-active interface. In contrast, if the F_1 and F_2 layers become parallel half-metals, the central f_C interface is similar to an ordinary spin-independent barrier and never makes any contribution to the phase ϕ_0 . It can be attributed to the phase cancellation of the spin-triplet pairs when they pass through the f_C interface. As a result, the current-phase relation is similar to that in the $S/f_L\text{-F-}f_R/S$ junction. The advantages of the $S/f_L\text{-F}_1\text{-}f_C\text{-F}_2\text{-}f_R/S$ junction and the possible experimental implementation are introduced in the Supplemental Material [66].

II. MODEL AND FORMULA

In general, Green's function technique is a very powerful tool for studying diffusive S/F systems. The quasiclassical approaches for Green's function were proposed by Eilenberger [67] and Usadel [68] successively. However, the applicability of these methods assumes that the exchange field h in the ferromagnet should be much smaller than the Fermi energy $h \ll E_F$ and the use of the Usadel equations implies even more restrictive conditions $h\tau \ll 1$, where τ is the electrons scattering time [2]. As a result, since the transport

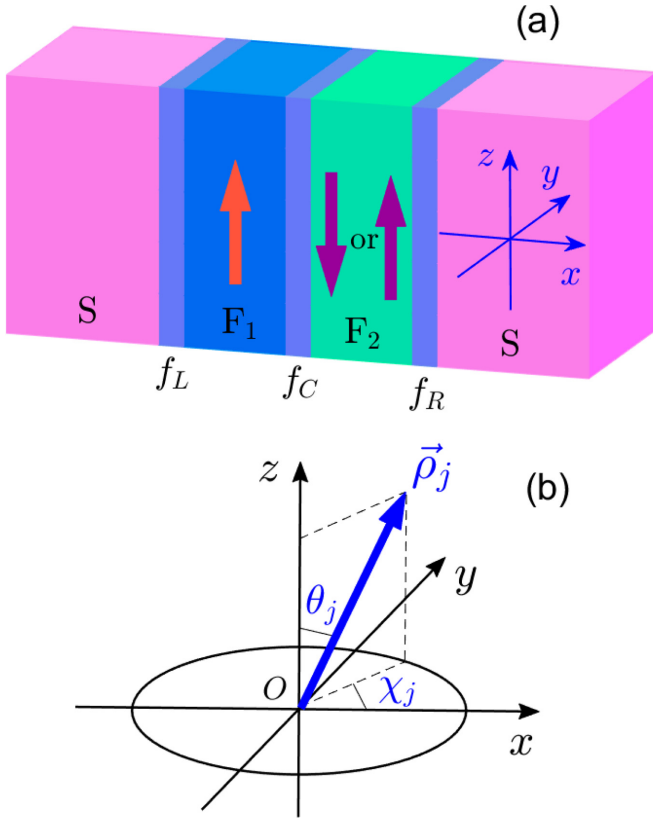


FIG. 1. (a) Schematic diagram of the $S/f_L\text{-}F_1\text{-}f_C\text{-}F_2\text{-}f_R/S$ junction, where thick arrows in F_1 and F_2 indicate the directions of the exchange field, and the thicknesses of F_1 and F_2 are d_1 and d_2 , respectively. The f_L , f_C , and f_R interfaces are assumed to be spin-active potential barriers due to misaligned local magnetizations. (b) The direction of magnetization $\vec{\rho}_j$ at the f_j interface, where $j = L, C$, and R correspond to the left, central, and right interfaces, respectively. θ_j and χ_j denote polar and azimuthal angles.

properties of the majority and minority electrons in the F layers are very different, the quasiclassical approaches lose their effectiveness, and some subtle qualitative effects may be missed, see, for example, [30,33,69,70]. Moreover, a lot of experimental activities with the S/F heterostructures deal with strong ferromagnets (or even half-metals [63,71,72]) for which the quasiclassical approximation cannot provide an adequate quantitative description. The alternative approach for the description of proximity effects in strong ferromagnets is the use of the microscopical approach based on the BdG equations [65]. For the inhomogeneous ferromagnetic Josephson junction, analytical solutions to the BdG equations are generally not easy to obtain. The exact numerical solutions of these equations may provide additional information to the quasiclassical approach and this method was used in [73–85] and references cited therein. In the following, we describe the generalized BdG method in detail.

The considered $S/f_L\text{-}F_1\text{-}f_C\text{-}F_2\text{-}f_R/S$ Josephson junction is shown schematically in Fig. 1. The x axis is chosen to be perpendicular to the layer interfaces with the origin located at the position of the f_C interface. The BCS mean-field effective

Hamiltonian is given by [2,65]

$$H_{\text{eff}} = \sum_{\alpha,\beta} \int d\mathbf{r} \left\{ \hat{\psi}_{\alpha}^{\dagger}(\mathbf{r}) [H_e - (h_z \hat{\sigma}_z)_{\alpha\alpha}] \hat{\psi}_{\alpha}(\mathbf{r}) + \frac{1}{2} [(i\hat{\sigma}_y)_{\alpha\beta} \Delta(\mathbf{r}) \hat{\psi}_{\alpha}^{\dagger}(\mathbf{r}) \hat{\psi}_{\beta}^{\dagger}(\mathbf{r}) + \text{H.c.}] - \hat{\psi}_{\alpha}^{\dagger}(\mathbf{r}) (\vec{\rho} \cdot \vec{\sigma})_{\alpha\beta} \hat{\psi}_{\beta}(\mathbf{r}) \right\}, \quad (1)$$

where $H_e = -\frac{\hbar^2 \nabla^2}{2m} - E_F$, and $\hat{\psi}_{\alpha}^{\dagger}(\mathbf{r})$ and $\hat{\psi}_{\alpha}(\mathbf{r})$ represent creation and annihilation operators with spin α . Here $\vec{\sigma} = (\hat{\sigma}_x, \hat{\sigma}_y, \hat{\sigma}_z)$ is the vector of Pauli matrices, m denotes the effective mass of the quasiparticles in both the superconductors and the ferromagnets, and E_F is the Fermi energy. We assume equal Fermi energies in the different regions of the junction. The superconducting gap is supposed to be constant in the superconducting electrodes and absent inside the ferromagnetic region:

$$\Delta(\mathbf{r}) = \begin{cases} \Delta e^{i\phi/2}, & x < -d_1, \\ 0, & -d_1 < x < d_2, \\ \Delta e^{-i\phi/2}, & x > d_2, \end{cases} \quad (2)$$

where Δ is the magnitude of the gap, and ϕ is the phase difference between the two superconducting electrodes. This approximation is justified when, for example, the thickness of the superconducting layers is much larger than the thickness of ferromagnetic layers. The exchange field in two ferromagnetic layers is parallel or antiparallel to the z axis. It has the form

$$h_z = \begin{cases} h_1 \hat{z}, & -d_1 < x < 0, \\ \pm h_2 \hat{z}, & 0 < x < d_2, \end{cases} \quad (3)$$

where \hat{z} is the unit vector along the z axis. We model the spin-active interface by a δ function potential barrier $\vec{\rho}(x) = \vec{\rho}_L \delta(x + d_1) + \vec{\rho}_C \delta(x) + \vec{\rho}_R \delta(x - d_2)$, where $\vec{\rho}_j$ ($j = L, C$ and R) is a vector parallel to the magnetization at the f_j interface. The components of $\vec{\rho}_j$ are characterized by the polar angle θ_j and the azimuthal angle χ_j in the usual way

$$\begin{aligned} \rho_j^x &= \rho_j \sin \theta_j \cos \chi_j, \\ \rho_j^y &= \rho_j \sin \theta_j \sin \chi_j, \\ \rho_j^z &= \rho_j \cos \theta_j, \end{aligned} \quad (4)$$

where ρ_j represents the strength of the interfacial magnetization.

To diagonalize the effective Hamiltonian H_{eff} , the field operator $\hat{\psi}_{\alpha}(\mathbf{r})$ is expanded utilizing the Bogoliubov transformation $\hat{\psi}_{\alpha}(\mathbf{r}) = \sum_n [u_{n\alpha}(\mathbf{r}) \hat{\gamma}_n + v_{n\alpha}^*(\mathbf{r}) \hat{\gamma}_n^{\dagger}]$, where $u_{n\alpha}$ and $v_{n\alpha}$ represent the quasiparticle amplitude, and $\hat{\gamma}_n$, $\hat{\gamma}_n^{\dagger}$ are the Bogoliubov annihilation and creation operators, respectively. Using the presentation $u_{n\alpha}(\mathbf{r}) = u_k^{\alpha} e^{ikx}$, $v_{n\alpha}(\mathbf{r}) = v_k^{\alpha} e^{ikx}$, the resulting BdG equations can be expressed as [65]

$$\begin{pmatrix} \hat{H}_0 + \hat{U} & i\hat{\sigma}_y \Delta(x) \\ -i\hat{\sigma}_y \Delta^*(x) & -\hat{H}_0 - \hat{U}^* \end{pmatrix} \begin{pmatrix} \hat{u}(x) \\ \hat{v}(x) \end{pmatrix} = \epsilon \begin{pmatrix} \hat{u}(x) \\ \hat{v}(x) \end{pmatrix}, \quad (5)$$

where

$$\hat{H}_0 = \begin{pmatrix} \xi_k - h_z & 0 \\ 0 & \xi_k + h_z \end{pmatrix},$$

$$\hat{U} = \hat{U}_L \delta(x + d_1) + \hat{U}_C \delta(x) + \hat{U}_R \delta(x - d_2),$$

and

$$\hat{U}_j = \begin{pmatrix} -\rho_j^z & -(\rho_j^x - i\rho_j^y) \\ -(\rho_j^x + i\rho_j^y) & \rho_j^z \end{pmatrix}.$$

Here $\xi_k = \frac{\hbar^2 k^2}{2m} - E_F$, and $\hat{u}(x) = [u_k^\uparrow(x) u_k^\downarrow(x)]^T$ and $\hat{v}(x) = [v_k^\uparrow(x) v_k^\downarrow(x)]^T$ are quasiparticle and quasihole wave functions, respectively.

The BdG equations (5) can be solved for each superconducting electrode and each ferromagnetic layer, respectively. For a given energy ϵ in the superconducting gap, we find the following plane-wave solutions in the left superconducting electrode:

$$\begin{aligned} \psi_L^S(x) = & C_1 \hat{\zeta}_1 e^{-ik_s^+ x} + C_2 \hat{\zeta}_2 e^{ik_s^- x} \\ & + C_3 \hat{\zeta}_3 e^{-ik_s^+ x} + C_4 \hat{\zeta}_4 e^{ik_s^- x}, \end{aligned} \quad (6)$$

where $k_s^\pm = k_F \sqrt{1 \pm i\sqrt{\Delta^2 - \epsilon^2}/E_F - (k_\parallel/k_F)^2}$ are the perpendicular components of the wave vectors for quasiparticles in both superconductors, and k_\parallel is the parallel component. $\hat{\zeta}_1 = [1 \ 0 \ 0 \ R_1 e^{-i\phi/2}]^T$, $\hat{\zeta}_2 = [1 \ 0 \ 0 \ R_2 e^{-i\phi/2}]^T$, $\hat{\zeta}_3 = [0 \ 1 \ -R_1 e^{-i\phi/2} \ 0]^T$, and $\hat{\zeta}_4 = [0 \ 1 \ -R_2 e^{-i\phi/2} \ 0]^T$ are the four basis wave functions of the left superconductor, in which $R_{1(2)} = (\epsilon \mp i\sqrt{\Delta^2 - \epsilon^2})/\Delta$. The corresponding wave function in the right superconducting electrode can be described by

$$\psi_R^S(x) = D_1 \hat{\eta}_1 e^{ik_s^+ x} + D_2 \hat{\eta}_2 e^{-ik_s^- x} + D_3 \hat{\eta}_3 e^{ik_s^+ x} + D_4 \hat{\eta}_4 e^{-ik_s^- x}, \quad (7)$$

where $\hat{\eta}_1 = [1 \ 0 \ 0 \ R_1 e^{i\phi/2}]^T$, $\hat{\eta}_2 = [1 \ 0 \ 0 \ R_2 e^{i\phi/2}]^T$, $\hat{\eta}_3 = [0 \ 1 \ -R_1 e^{i\phi/2} \ 0]^T$, and $\hat{\eta}_4 = [0 \ 1 \ -R_2 e^{i\phi/2} \ 0]^T$.

The wave function in the F_1 layer is

$$\begin{aligned} \psi_1(x) = & (M_1 e^{ik_1 x} + M_1' e^{-ik_1 x}) \hat{e}_1 + (M_2 e^{ik_2 x} + M_2' e^{-ik_2 x}) \hat{e}_2 \\ & + (M_3 e^{ik_3 x} + M_3' e^{-ik_3 x}) \hat{e}_3 + (M_4 e^{ik_4 x} + M_4' e^{-ik_4 x}) \hat{e}_4, \end{aligned} \quad (8)$$

where $\hat{e}_1 = (1 \ 0 \ 0 \ 0)^T$, $\hat{e}_2 = (0 \ 1 \ 0 \ 0)^T$, $\hat{e}_3 = (0 \ 0 \ 1 \ 0)^T$, and $\hat{e}_4 = (0 \ 0 \ 0 \ 1)^T$ are basis wave functions in the ferromagnetic region, and $k_{1(2)} = k_F \sqrt{1 + (\epsilon \pm h_1)/E_F - (k_\parallel/k_F)^2}$ and $k_{3(4)} = k_F \sqrt{1 - (\epsilon \mp h_1)/E_F - (k_\parallel/k_F)^2}$ are the perpendicular components of the wave vectors for the quasiparticles in the F_1 layer. The corresponding wave function $\psi_2(x)$ in the F_2 layer can be derived from Eq. (8) by replacement $h_1 \rightarrow h_2$. It is worthy to note that the parallel component k_\parallel is conserved in the transport processes of the quasiparticles.

The wave functions $[\psi_L^S(x), \psi_1(x), \psi_2(x), \text{ and } \psi_R^S(x)]$ and their first derivatives satisfy the following boundary conditions:

$$\begin{aligned} \psi_L^S(-d_1) &= \psi_1(-d_1), \\ \psi_1'(-d_1) - \psi_L^{S'}(-d_1) &= k_F \begin{pmatrix} \hat{V}_L & 0 \\ 0 & \hat{V}_L^* \end{pmatrix} \psi(-d_1), \end{aligned} \quad (9)$$

$$\psi_1(0) = \psi_2(0),$$

$$\psi_2'(0) - \psi_1'(0) = k_F \begin{pmatrix} \hat{V}_C & 0 \\ 0 & \hat{V}_C^* \end{pmatrix} \psi(0), \quad (10)$$

$$\psi_2(d_2) = \psi_R^S(d_2),$$

$$\psi_R^{S'}(d_2) - \psi_2'(d_2) = k_F \begin{pmatrix} \hat{V}_R & 0 \\ 0 & \hat{V}_R^* \end{pmatrix} \psi(d_2), \quad (11)$$

where

$$\hat{V}_j = \begin{pmatrix} -P_j^z & -(P_j^x - iP_j^y) \\ -(P_j^x + iP_j^y) & P_j^z \end{pmatrix}. \quad (12)$$

We define the dimensionless spin-dependent parameter $(P_j^x, P_j^y, P_j^z) = P_j(\sin \theta_j \cos \chi_j, \sin \theta_j \sin \chi_j, \cos \theta_j)$, where the dimensionless parameter $P_j = 2m\rho_j/(\hbar^2 k_F)$ describes the strength of the spin-active barrier at the f_j interface.

From these boundary conditions, we can set up 24 linear equations in the following form:

$$\hat{A}X = \hat{B}, \quad (13)$$

where X contains 24 scattering coefficients, and \hat{A} is a 24×24 matrix. The solution of the characteristic equation

$$\det \hat{A} = 0 \quad (14)$$

allows one to identify two Andreev bound-state solutions for energies $E_{A\omega}$ ($\omega = 1, 2$). Below we will consider the case of the short Josephson junction with a thickness much smaller than the superconducting coherence length ξ_S . In such a case, the contribution to the Josephson current comes from the discrete Andreev bound states, and the continuous electron state does not play any role (see, e.g., [86,87]). In a one-dimensional (1D) structure, the Josephson current can be calculated by the general formula

$$I^{1D}(\phi) = \frac{2e}{\hbar} \frac{\partial \Omega}{\partial \phi}, \quad (15)$$

where Ω is the phase-dependent thermodynamic potential. This potential arises from the excitation spectrum by using the formula [88,89]

$$\Omega = -2T \sum_{\omega} \ln \left[2 \cosh \frac{E_{A\omega}(\phi)}{2T} \right], \quad (16)$$

where Δ , h_1 , h_2 , P_j , θ_j , and χ_j are assumed to be the equilibrium values, which minimize the free energy of the $S/f_L\text{-}F_1\text{-}f_C\text{-}F_2\text{-}f_R/S$ junction and depend on microscopic parameters [90]. The summation in (16) is taken over all positive Andreev energies $[0 < E_{A\omega}(\phi) < \Delta]$. For each value of ϕ , we solve Eq. (14) numerically to obtain the two spin-polarized Andreev levels. Since the Andreev energy spectra are doubled as they include the Bogoliubov redundancy, and only half of the energy states should be taken into account, we can find the 1D Josephson current via Eqs. (15) and (16).

In a three-dimensional (3D) case, the Josephson current can be expressed as [70]

$$I^{3D}(\phi) = \frac{4\pi \Delta}{eR_N} \int_0^1 I^{1D}(\tilde{k}_\parallel) \tilde{k}_\parallel d\tilde{k}_\parallel, \quad (17)$$

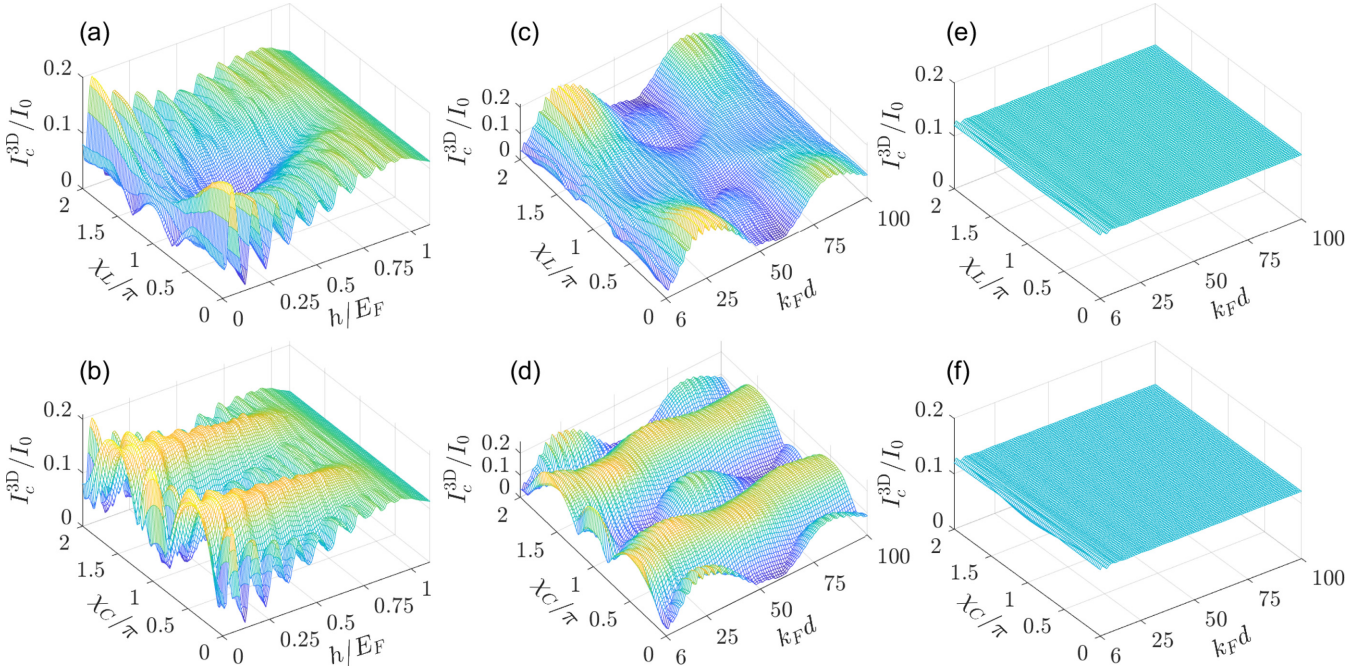


FIG. 2. The critical current I_c^{3D} versus the left azimuthal angle χ_L for $\chi_C = \chi_R = 0$ [(a), (c), and (e)], and I_c^{3D} versus χ_C for $\chi_L = \chi_R = 0$ [(b), (d), and (f)]. Here it is shown that I_c^{3D} varies with the exchange field h/E_F for the ferromagnetic thickness $k_F d = 50$ [(a) and (b)], and I_c^{3D} varies with $k_F d$ for $h/E_F = 0.1$ [(c) and (d)] and $h/E_F = 1.05$ [(e) and (f)]. In all panels, the spin-active barriers are taken as $P_L = P_R = 1$ and $P_C = 1.5$.

where $R_N^{-1} = e^2 k_F^2 S / (4\pi^2 \hbar)$ is the Sharvin resistance, and $\tilde{k}_{\parallel} = k_{\parallel} / k_F$ is the normalized wave vector. The 3D critical current can be derived from $I_c^{3D} = \max_{\phi} |I^{3D}(\phi)|$.

III. RESULTS AND DISCUSSIONS

In our calculations we use the superconducting gap Δ as a unit of energy and take the Fermi energy $E_F = 1000\Delta$. All length scales and the exchange field strengths are normalized by the inverse Fermi wave-vector k_F and the Fermi energy E_F , respectively. Note that the approximation of the short Josephson junction ($k_F d_1, k_F d_2 \ll 1000$) is fully satisfied in the presented calculations. The normalized unit of current is $I_0 = 2\pi \Delta / (e R_N)$ in the 3D case. The calculations of all the currents are performed at temperature $T = 0$ throughout the paper.

For simplicity, we define that the magnetization vector $\vec{\rho}_j$ at the f_j interface lies in the x - y plane ($\theta_L = \theta_C = \theta_R = \pi/2$), and sets up the azimuthal angle χ_j with the x axis, see Fig. 1. The magnetization of the F_1 layer is fixed along the z axis, and the direction of the F_2 layer is antiparallel or parallel to the F_1 layer. Unless otherwise stated, the results are calculated for the same strength of exchange fields ($h_1 = \pm h_2 = h$) and the same thicknesses ($d_1 = d_2 = d$) in the F_1 and F_2 layers.

A. The Josephson current in the S/ f_L - F_1 - f_C - F_2 - f_R /S junction with antiparallel magnetization configurations

We discuss first the Josephson current for the antiparallel magnetic configurations ($h_1 = -h_2 = h$). As illustrated in Figs. 2(a) and 2(c), I_c^{3D} exhibits an oscillatory characteristic with increasing h/E_F and $k_F d$. The oscillating effect of I_c^{3D}

is more prominent at $\chi_L = 0$ and 2π but almost no longer appears at $\chi_L = \pi$. Figures 2(b) and 2(d) show that when χ_C takes values around 0.5π and 1.5π , I_c^{3D} always maintains a large amplitude over the entire range of h/E_F and $k_F d$. As χ_C is in the vicinity of 0 , π , and 2π , the I_c^{3D} amplitude decreases, but its oscillatory character with h/E_F and $k_F d$ becomes more pronounced. For the half-metallic ferromagnet in Figs. 2(e) and 2(f), I_c^{3D} neither changes with the azimuthal angles χ_L and χ_C nor with the ferromagnetic thickness $k_F d$. These features demonstrate that the Josephson current through the system is a long-range spin-polarized supercurrent. Moreover, the left and right interfaces play the same role in the transport process of the Josephson current. The variation of the Josephson current with the two interface angles (χ_L and χ_R) is described in the Supplemental Material [66].

Continually, we explore the dependence of the Josephson current on the interfacial barriers and the ferromagnetic exchange fields. As shown in Fig. 3(a), without the spin-active barriers ($P_L = 0$ or/and $P_C = 0$), I_c^{3D} is zero. As the interfacial barriers increase, I_c^{3D} increases rapidly and reaches a maximum for $P_L = 1$ and $P_C = 1.5$, then decreases at larger values of P_L and P_C . The decrease in I_c^{3D} at large P_L and P_C signals that the interfacial barriers not only flip the electron spin but also suppress the transport of paired electrons. By contrast, as illustrated in Fig. 3(b), I_c^{3D} shows the same dependence on the left and right barriers and reaches a maximum at $P_L = P_R = 1$. On the other hand, Fig. 3(c) shows the dependence of $I^{3D}(\phi)$ on h/E_F , when the f_L interface is magnetized along the y axis, and the other two interfaces are along the x axis. Under a weak h/E_F , $I^{3D}(\phi)$ cannot be represented as a sinusoidal function. But when h/E is strong enough, the current satisfies a relation $I^{3D}(\phi) = I_c^{3D} \sin(\phi - \pi/2)$ for $\chi_L = \pi/2$. When the f_C

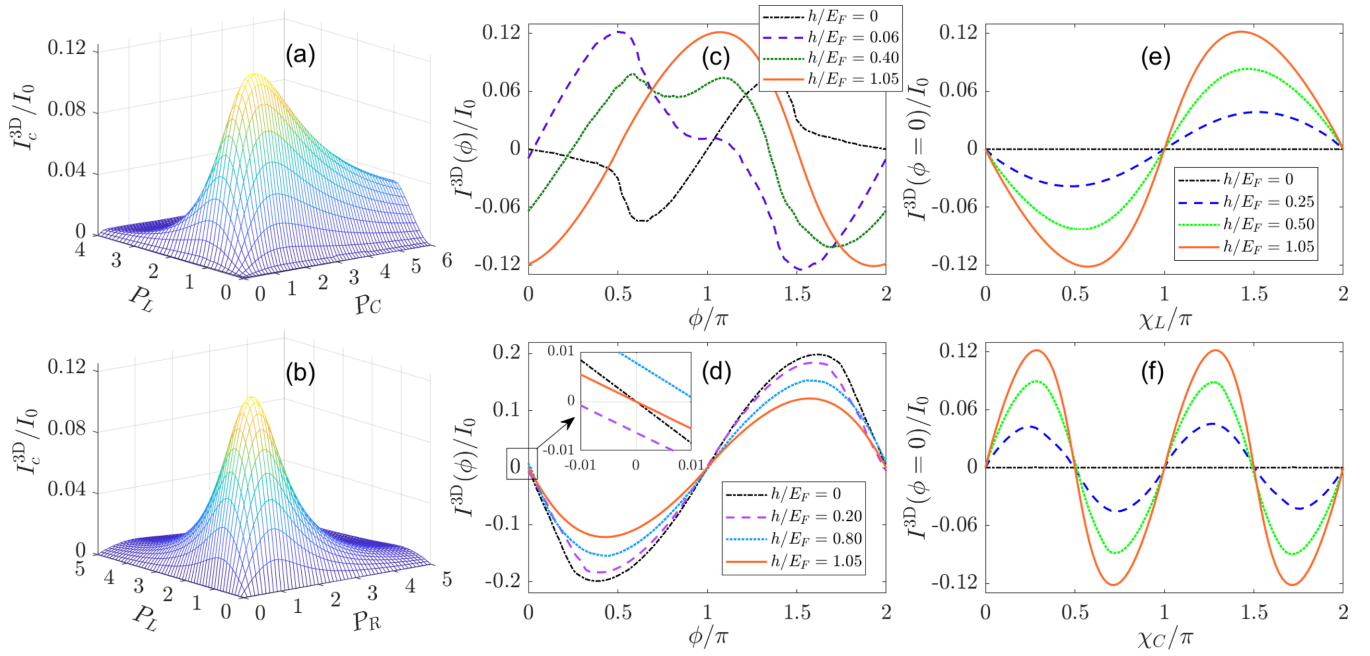


FIG. 3. The critical current I_c^{3D} versus the strength of the spin-active barriers P_L and P_C in the case of $P_L = P_R$ (a), and I_c^{3D} versus P_L and P_R for $P_C = 1.5$ (b). In (a) and (b) we choose $h/E_F = 1.05$, $k_F d = 50$, $\chi_L = \chi_R = 0$, and $\chi_C = \pi/2$. Current-phase relation $I^{3D}(\phi)$ under different exchange fields h/E_F for $\chi_L = \pi/2$ when $\chi_C = \chi_R = 0$ (c) and for $\chi_C = \pi/2$ when $\chi_L = \chi_R = 0$ (d). Spontaneous supercurrent $I^{3D}(\phi = 0)$ versus χ_L for $\chi_C = \chi_R = 0$ (e), and $I^{3D}(\phi = 0)$ versus χ_C for $\chi_L = \chi_R = 0$ (f) when h/E_F takes several values. (e) and (f) use the same legends. In (c)–(f) we choose $k_F d = 50$, $P_L = P_R = 1$, and $P_C = 1.5$.

interface is oriented along the y axis, the $I^{3D}(\phi)$ amplitude gradually decreases with increasing h/E_F , but the current approximately maintains a sinusoidal relation $I^{3D}(\phi) = I_c^{3D} \sin(\phi + \pi)$ for $\chi_C = \pi/2$ [see Fig. 3(d)]. In comparison, as shown in Figs. 3(e) and 3(f), $I^{3D}(\phi = 0)$ does not exist at $h/E_F = 0$, and its amplitude increases with increasing h/E_F . As the two ferromagnets are converted into half-metals, the amplitude reaches the maximum. The oscillation periods of $I^{3D}(\phi = 0)$ with angles χ_L and χ_C are 2π and π , respectively. Therefore, the spontaneous supercurrent satisfies the following relations: $I^{3D}(\phi = 0) = I_c^{3D} \sin(-\chi_L)$ for $\chi_C = \chi_R = 0$ and $I^{3D}(\phi = 0) = I_c^{3D} \sin(2\chi_C)$ for $\chi_L = \chi_R = 0$.

Next, we show the current-phase relation $I^{3D}(\phi)$ and the spontaneous supercurrent $I^{3D}(\phi = 0)$ for the half-metallic phase in Fig. 4. It can be seen that the oscillation period of current with χ_L and χ_R is twice that with χ_C . According to the inference described in the Supplemental Material [66], we can deduce a complete current-phase relation $I^{3D}(\phi) = I_c^{3D} \sin(\phi + 2\chi_C - \chi_L - \chi_R)$ for the entire system.

We now give a simple physical picture to describe the propagation process of the Cooper pairs in the $S/f_L-F_1-f_C-F_2-f_R/S$ junction when the F_1 and F_2 layers are antiparallel half-metals. As mentioned before, the orientation of the interfacial barrier is characterized by the polar (θ) and the azimuthal (χ) angles measured from the z axis in spin space. The transformation formulas for basis vectors quantized along the direction (θ, χ) in terms of basis vectors quantized along the z axis read [6]

$$(\uparrow)_{\theta, \chi} = \cos \frac{\theta}{2} e^{-i\frac{\chi}{2}} (\uparrow)_z + \sin \frac{\theta}{2} e^{i\frac{\chi}{2}} (\downarrow)_z, \quad (18a)$$

$$(\downarrow)_{\theta, \chi} = -\sin \frac{\theta}{2} e^{-i\frac{\chi}{2}} (\uparrow)_z + \cos \frac{\theta}{2} e^{i\frac{\chi}{2}} (\downarrow)_z, \quad (18b)$$

and can be used to find the transformation for the spin-singlet pairs and the spin-triplet pairs [6]

$$(\uparrow\downarrow - \downarrow\uparrow)_{\theta, \chi} = (\uparrow\downarrow - \downarrow\uparrow)_z, \quad (19a)$$

$$(\uparrow\downarrow + \downarrow\uparrow)_{\theta, \chi} = -\sin \theta [e^{-i\chi} (\uparrow\downarrow)_z - e^{i\chi} (\downarrow\uparrow)_z] + \cos \theta (\uparrow\downarrow + \downarrow\uparrow)_z. \quad (19b)$$

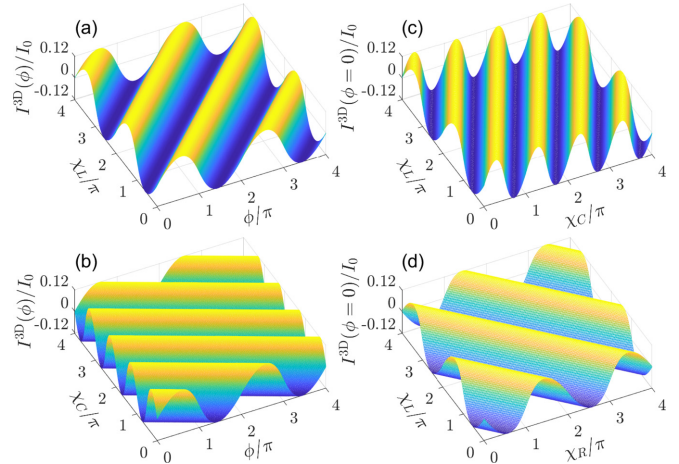


FIG. 4. Current-phase relation $I^{3D}(\phi)$ versus the azimuthal angles χ_L (a) and χ_C (b). Spontaneous supercurrent $I^{3D}(\phi = 0)$ versus the azimuthal angles (χ_L, χ_C) (c) and (χ_L, χ_R) (d). Here the unlabeled azimuthal angles in each panel are set to 0, and the parameters are as follows: $h/E_F = 1.05$, $k_F d = 50$, $P_L = P_R = 1$, and $P_C = 1.5$.

The reverse transformation formulas can be written as

$$(\uparrow)_z = \cos \frac{\theta}{2} e^{i\frac{\chi}{2}} (\uparrow)_{\theta, \chi} - \sin \frac{\theta}{2} e^{i\frac{\chi}{2}} (\downarrow)_{\theta, \chi}, \quad (20a)$$

$$(\downarrow)_z = \sin \frac{\theta}{2} e^{-i\frac{\chi}{2}} (\uparrow)_{\theta, \chi} + \cos \frac{\theta}{2} e^{-i\frac{\chi}{2}} (\downarrow)_{\theta, \chi}, \quad (20b)$$

in which case the quantization direction of the basis vector rotates from the z axis to the orientation (θ, χ) . So the spin-triplet pairs have the following transformation:

$$(\uparrow\uparrow)_z = e^{i\chi} \left[\cos^2 \frac{\theta}{2} (\uparrow\uparrow)_{\theta, \chi} + \sin^2 \frac{\theta}{2} (\downarrow\downarrow)_{\theta, \chi} \right] - \sin \frac{\theta}{2} \cos \frac{\theta}{2} e^{i\chi} (\uparrow\downarrow + \downarrow\uparrow)_{\theta, \chi}, \quad (21a)$$

$$(\downarrow\downarrow)_z = e^{-i\chi} \left[\sin^2 \frac{\theta}{2} (\uparrow\uparrow)_{\theta, \chi} + \cos^2 \frac{\theta}{2} (\downarrow\downarrow)_{\theta, \chi} \right] + \sin \frac{\theta}{2} \cos \frac{\theta}{2} e^{-i\chi} (\uparrow\downarrow + \downarrow\uparrow)_{\theta, \chi}. \quad (21b)$$

The transport process of the Cooper pairs in the $S/f_L-F_1-f_C-F_2-f_R/S$ junction can be divided into the following steps:

(i) It is well known that, since the spin-singlet pairs $(\uparrow\downarrow - \downarrow\uparrow)$ penetrate from the left superconductor into the f_L interfacial region, it induces a mixture of the spin-singlet pairs $(\uparrow\downarrow - \downarrow\uparrow)_{\theta_L, \chi_L}$ and the spin-triplet pairs $(\uparrow\downarrow + \downarrow\uparrow)_{\theta_L, \chi_L}$ in the f_L region [5]. When the magnetization direction of the F_1 layer is different from that in the f_L interface, the spin-singlet pairs $(\uparrow\downarrow - \downarrow\uparrow)_{\theta_L, \chi_L}$, which are rotationally invariant, cannot survive in the F_1 layer due to the strong exchange field. But the spin-triplet pairs $(\uparrow\downarrow + \downarrow\uparrow)_{\theta_L, \chi_L}$ can be transformed into a combination of the equal-spin-triplet pairs and the opposite-spin-triplet pairs when viewed with respect to the z axis, see formula (19b). Because the magnetization in the interfaces lies in the x - y plane ($\theta_L = \theta_C = \theta_R = \pi/2$), the spin-triplet pairs $(\uparrow\downarrow + \downarrow\uparrow)_z$ disappear due to former factor $\cos \theta = 0$. Moreover, the F_1 layer is defined as being polarized along the z axis. So the spin-triplet pairs $(\uparrow\uparrow)_z$ can survive in the F_1 layer, but the spin-triplet pairs $(\downarrow\downarrow)_z$ are not allowed. When the spin-triplet pairs transfer from the f_L interface into the F_1 layer, a conversion process can be obtained:

$$(\uparrow\downarrow + \downarrow\uparrow)_{\theta_L, \chi_L} \longrightarrow -e^{-i\chi_L} (\uparrow\uparrow)_z. \quad (22)$$

(ii) When the spin-triplet pairs pass from the F_1 layer into the f_C interface, they have a transition process

$$(\uparrow\uparrow)_z = \frac{1}{2} e^{i\chi_C} [(\uparrow\uparrow)_{\theta_C, \chi_C} + (\downarrow\downarrow)_{\theta_C, \chi_C}] - \frac{1}{2} e^{i\chi_C} (\uparrow\downarrow + \downarrow\uparrow)_{\theta_C, \chi_C}. \quad (23)$$

If one ignores the contribution of the first term on the right-hand side of Eq. (23), a simplified process can be obtained:

$$(\uparrow\uparrow)_z \longrightarrow -\frac{1}{2} e^{i\chi_C} (\uparrow\downarrow + \downarrow\uparrow)_{\theta_C, \chi_C}. \quad (24)$$

(iii) Following the above process, the spin-triplet pairs transport from the f_C interface into the F_2 layer, in which case they undergo a transformation

$$(\uparrow\downarrow + \downarrow\uparrow)_{\theta_C, \chi_C} = -e^{-i\chi_C} (\uparrow\uparrow)_z + e^{i\chi_C} (\downarrow\downarrow)_z. \quad (25)$$

Because the magnetization of the F_2 layer is antiparallel to the z axis, the spin-triplet pairs $(\uparrow\uparrow)_z$ will be completely

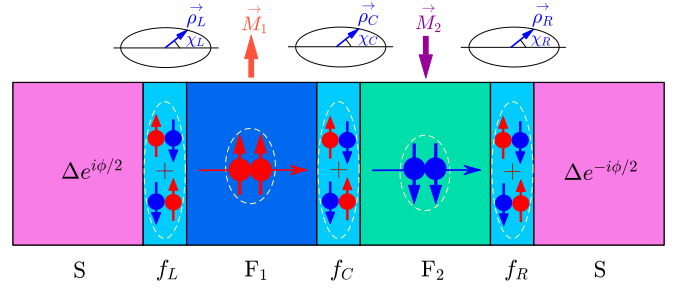


FIG. 5. Transformation process of the spin-triplet pairs in the $S/f_L-F_1-f_C-F_2-f_R/S$ junction. The F_1 and F_2 are strongly spin-polarized half-metals with antiparallel magnetizations \vec{M}_1 and \vec{M}_2 , and the interfacial barriers f_L , f_C , and f_R have misaligned magnetizations $\vec{\rho}_L$, $\vec{\rho}_C$, and $\vec{\rho}_R$. The azimuthal angles of $\vec{\rho}_L$, $\vec{\rho}_C$, and $\vec{\rho}_R$ are denoted by χ_L , χ_C , and χ_R , respectively. The spin-triplet pairs $(\uparrow\downarrow + \downarrow\uparrow)$ are usually generated in the f_L , f_C , and f_R regions, which can be converted to the equal-spin-triplet pairs $(\uparrow\uparrow)$ in the F_1 layer or $(\downarrow\downarrow)$ in the F_2 layer. When the spin-triplet pairs transport from the left f_L region to the right f_R region, they will acquire an additional phase $2\chi_C - \chi_L - \chi_R$.

suppressed. As a result, we have a transformation process:

$$(\uparrow\downarrow + \downarrow\uparrow)_{\theta_C, \chi_C} \longrightarrow e^{i\chi_C} (\downarrow\downarrow)_z. \quad (26)$$

(iv) When the spin-triplet pairs move from the F_2 layer to the f_R interface, they experience a transformation process:

$$(\downarrow\downarrow)_z = \frac{1}{2} e^{-i\chi_R} [(\uparrow\uparrow)_{\theta_R, \chi_R} + (\downarrow\downarrow)_{\theta_R, \chi_R}] + \frac{1}{2} e^{-i\chi_R} (\uparrow\downarrow + \downarrow\uparrow)_{\theta_R, \chi_R}. \quad (27)$$

If the first term on the right-hand side of Eq. (27) is omitted, the following result can be achieved:

$$(\downarrow\downarrow)_z \longrightarrow \frac{1}{2} e^{-i\chi_R} (\uparrow\downarrow + \downarrow\uparrow)_{\theta_R, \chi_R}. \quad (28)$$

The transmission process of the spin-triplet pairs through the entire $S/f_L-F_1-f_C-F_2-f_R/S$ junction can be summarized as

$$(\uparrow\downarrow + \downarrow\uparrow)_{\theta_L, \chi_L} \xrightarrow{f_L \Rightarrow F_1} -e^{-i\chi_L} (\uparrow\uparrow)_z \xrightarrow{F_1 \Rightarrow f_C} e^{i(\chi_C - \chi_L)} (\uparrow\downarrow + \downarrow\uparrow)_{\theta_C, \chi_C} \xrightarrow{f_C \Rightarrow F_2} e^{i(2\chi_C - \chi_L)} (\downarrow\downarrow)_z \xrightarrow{F_2 \Rightarrow f_R} e^{i(2\chi_C - \chi_L - \chi_R)} (\uparrow\downarrow + \downarrow\uparrow)_{\theta_R, \chi_R}, \quad (29)$$

where we discard the factors in front of the spin-triplet pairs. The above process is illustrated visually in Fig. 5. The spin-triplet pairs acquire an additional phase $2\chi_C - \chi_L - \chi_R$ when they pass through the entire system. The obtained phase may directly enter into the current phase to produce an expression $I^{3D}(\phi) = I_c^{3D} \sin(\phi + 2\chi_C - \chi_L - \chi_R)$. This qualitative interpretation is consistent with the numerical results we obtained above.

B. The Josephson current in the $S/f_L-F_1-f_C-F_2-f_R/S$ junction with parallel magnetization configurations

In the following we investigate the contribution of the interfacial azimuthal angles to the Josephson current when the F_1 and F_2 layers are parallel half-metals ($h_1 = h_2 = h$ and $h/E_F = 1.05$). The top row of Fig. 6 shows the dependence of the current-phase relation $I^{3D}(\phi)$ on the azimuthal angles.

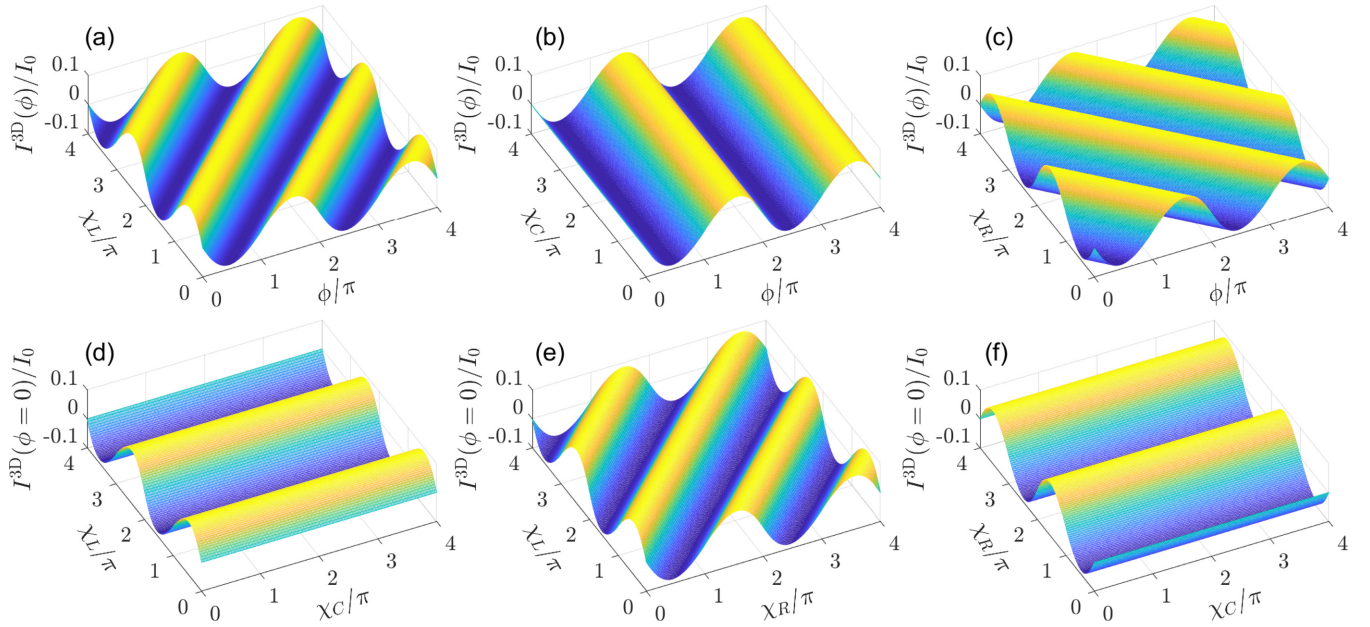


FIG. 6. The top row illustrates the current-phase relation $I^{3D}(\phi)$ as a function of the azimuthal angles χ_L (a), χ_C (b), and χ_R (c). The bottom row shows the spontaneous supercurrent $I^{3D}(\phi = 0)$ as a function of (χ_L, χ_C) (d), (χ_L, χ_R) (e), and (χ_R, χ_C) (f). The unlabeled azimuthal angles in each panel take the value of 0, and the other parameters are $h/E_F = 1.05$, $k_F d = 50$, $P_L = P_R = 1$, and $P_C = 1.5$. The results shown are for the $S/f_L-F_1-f_C-F_2-f_R/S$ junction with parallel magnetizations.

As seen, $I^{3D}(\phi)$ oscillates with χ_L and χ_R but does not vary with χ_C . The current magnitude is reduced compared to that in the junction with the antiparallel magnetizations. Moreover, the bottom row of Fig. 6 presents the influence of the azimuthal angles on the spontaneous supercurrent $I^{3D}(\phi = 0)$. It is observed that χ_C has no contribution to $I^{3D}(\phi = 0)$. The variation characteristic of $I^{3D}(\phi = 0)$ with χ_L is different from that in the antiparallel $S/f_L-F_1-f_C-F_2-f_R/S$ junction. From the dependence of the current on the phase difference and the azimuthal angles, one can deduce a current-phase relation $I^{3D}(\phi) = I_c^{3D} \sin(\phi + \chi_R - \chi_L + \pi)$.

The physical picture leading to this relation can be explained by the transport process of the spin-triplet pairs:

$$\begin{aligned}
 (\uparrow\downarrow + \downarrow\uparrow)_{\theta_L, \chi_L} &\xrightarrow{f_L \Rightarrow F_1} -e^{-i\chi_L} (\uparrow\uparrow)_z \xrightarrow{F_1 \Rightarrow f_C} \\
 e^{i(\chi_C - \chi_L)} (\uparrow\downarrow + \downarrow\uparrow)_{\theta_C, \chi_C} &\xrightarrow{f_C \Rightarrow F_2} -e^{-i\chi_L} (\uparrow\uparrow)_z \\
 \xrightarrow{F_2 \Rightarrow f_R} &e^{i(\chi_R - \chi_L)} (\uparrow\downarrow + \downarrow\uparrow)_{\theta_R, \chi_R}.
 \end{aligned} \quad (30)$$

In the above process, when the spin-triplet pairs pass from the F_1 layer into the f_C interface, they transform from $(\uparrow\uparrow)_z$ to $(\uparrow\downarrow + \downarrow\uparrow)_{\theta_C, \chi_C}$ and acquire an additional phase χ_C . Continually, if $(\uparrow\downarrow + \downarrow\uparrow)_{\theta_C, \chi_C}$ penetrate from the f_C interface into the F_2 layer, they are converted into $(\uparrow\uparrow)_z$ and get another phase $-\chi_C$. The two phases resulting from the spin-triplet pairs crossing the f_C interface can superimpose and cancel each other out. During the entire transmission process, the obtained phase is only related to the azimuthal angles χ_L and χ_R . So we can say that the f_C interface works as a conventional potential barrier and does not contribute any additional phase to the Josephson current. The above current characteristics are the same as those in the $S/f_L-F-f_R/S$ junction, which we further demonstrate below.

C. The Josephson current in the $S/f_L-F-f_R/S$ junction

In Figs. 7(a) and 7(b) we illustrate the variation of the current-phase relation $I^{3D}(\phi)$ with the azimuthal angles χ_L and χ_R in the $S/f_L-F-f_R/S$ junction. It can be seen that, except for the increased amplitude, $I^{3D}(\phi)$ has the same characteristics as shown in Figs. 6(a) and 6(c). Moreover, Fig. 7(c) shows the spontaneous current $I^{3D}(\phi = 0)$ as a function of the azimuthal angles χ_L and χ_R , which is the same as that shown in Fig. 6(e). These behaviors demonstrate that the Josephson current in the $S/f_L-F-f_R/S$ junction satisfies a relation $I^{3D}(\phi) = I_c^{3D} \sin(\phi + \chi_R - \chi_L + \pi)$, which is consistent with the results in Refs. [6,22,23]. This relation can be explained by the transport process of the spin-triplet pairs:

$$\begin{aligned}
 (\uparrow\downarrow + \downarrow\uparrow)_{\theta_L, \chi_L} &\xrightarrow{f_L \Rightarrow F} -e^{-i\chi_L} (\uparrow\uparrow)_z \xrightarrow{F \Rightarrow f_R} \\
 e^{i(\chi_R - \chi_L)} (\uparrow\downarrow + \downarrow\uparrow)_{\theta_R, \chi_R}.
 \end{aligned} \quad (31)$$

Therefore, the same current-phase relation can be generated in the $S/f_L-F-f_R/S$ junction and the parallel $S/f_L-F_1-f_C-F_2-f_R/S$ junction. The last which must be noted is that the current magnitude in the $S/f_L-F-f_R/S$ junction is almost the same as that in the antiparallel $S/f_L-F_1-f_C-F_2-f_R/S$ junction (see Figs. 4 and 7). It indicates that adding the antiparallel F_2 layer and the f_C interface does not significantly suppress the Josephson current.

IV. CONCLUSION

On the basis of the exact numerical solution of the Bogoliubov-de Gennes equations, we have investigated the Josephson current in the $S/f_L-F_1-f_C-F_2-f_R/S$ junction. If the magnetizations of the F_1 and F_2 layers are antiparallel, the critical current oscillates with the exchange field and the thickness of the F_1 and F_2 layers when the

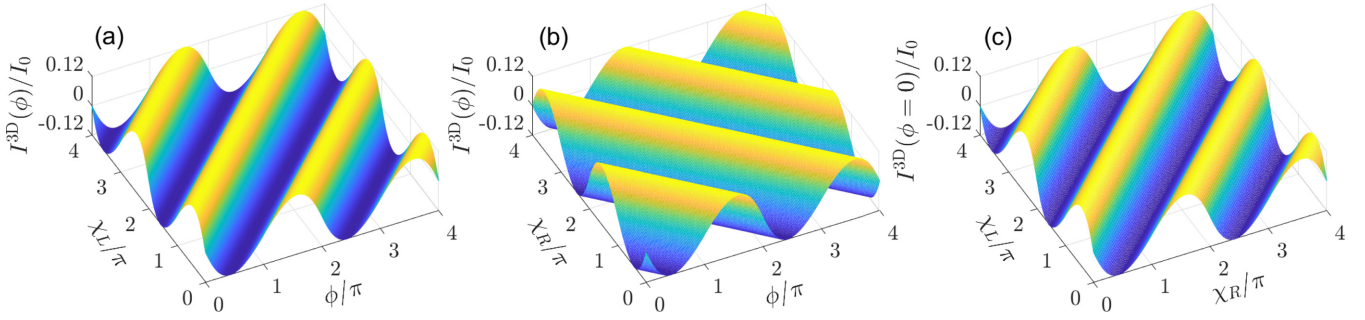


FIG. 7. Current-phase relation $I^{3D}(\phi)$ is shown as a function of the azimuthal angles χ_L (a) and χ_R (b). The spontaneous supercurrent $I^{3D}(\phi = 0)$ is shown as a function of the azimuthal angles (χ_L, χ_R) (c). The unlabeled azimuthal angles in each panel are taken as 0, and the other parameters are set to $h_1/E_F = 1.05$, $k_F d_1 = 50$, and $P_L = P_R = 1$. The results shown are for the S/f_L - F - f_R/S junction ($k_F d_2 = 0$ and $P_C = 0$).

azimuthal angle χ_L takes some specific values. The oscillation is not significant for the other χ_L . By contrast, when the magnetization at the f_C interface is perpendicular to that at the f_L and f_R interfaces, the critical current reaches a larger value and is rarely affected by the exchange field and the thickness. For other directions of the f_C interface, the critical current decreases and a significant oscillation effect occurs. Interestingly, the critical current will no longer change with the azimuthal angles and the ferromagnetic thickness once the antiparallel ferromagnets increase up to the half-metallic phase. In this situation, the Josephson current will gain an additional phase ϕ_0 to form an anomalous supercurrent $I^{3D}(\phi) = I_c^{3D} \sin(\phi + \phi_0)$ with $\phi_0 = 2\chi_C - \chi_L - \chi_R$. This feature reveals direct coupling between the interface magnetizations and the Josephson phase difference. We attribute this anomalous effect to the phase superposition. The spin-triplet pairs capture a phase as they pass through each interface. All the captured phases are superposed to contribute to the Josephson current. When the F_1 and F_2 layers become parallel half-metals, the central f_C interface cannot provide any phase to the Josephson current and $\phi_0 = \chi_R - \chi_L + \pi$. The f_C interface works like a conventional potential barrier because the spin-triplet pairs passing through the f_C interface create a phase cancellation effect. In such a case, the current-phase relation

is the same as that in the S/f_L - F - f_R/S junction. The results we obtained above might be used in experiments to construct novel structures to manufacture the ϕ_0 junction, and ultimately achieve the purpose of controlling the superconducting phase in superconducting spintronics.

ACKNOWLEDGMENTS

The authors thank A. I. Buzdin for useful discussions and suggestions. This work was supported by the National Natural Science Foundation of China (Grants No. 12174238 and No. 11604195), the Special Foundation for Theoretical Physics Research Program of China (Grant No. 11747035), the Natural Science Basic Research Program of Shaanxi (Programs No. 2020JM-597 and No. 2021JQ-748), and the Scientific Research Foundation of Shaanxi University of Technology (Grant No. SLGKY2006). J. Wu was supported by Natural Science Foundation of Guangdong Province (Grants No. 2017B030308003 and No. 2019B121203002), Guangdong Innovative and Entrepreneurial Research Team Program (No. 2016ZT06D348) and Science, Technology, and Innovation Commission of Shenzhen Municipality (Grants No. KYTDPT20181011104202253 and No. JCYJ20170412152620376).

-
- [1] A. A. Golubov, M. Yu. Kupriyanov, and E. Ilichev, The current-phase relation in Josephson junctions, *Rev. Mod. Phys.* **76**, 411 (2004).
 - [2] A. I. Buzdin, Proximity effects in superconductor-ferromagnet heterostructures, *Rev. Mod. Phys.* **77**, 935 (2005).
 - [3] F. S. Bergeret, A. F. Volkov, and K. B. Efetov, Odd triplet superconductivity and related phenomena in superconductor-ferromagnet structures, *Rev. Mod. Phys.* **77**, 1321 (2005).
 - [4] J. Linder and J. W. A. Robinson, Superconducting spintronics, *Nat. Phys.* **11**, 307 (2015).
 - [5] M. Eschrig, Spin-polarized supercurrents for spintronics, *Phys. Today* **64**(1), 43 (2011).
 - [6] M. Eschrig, Spin-polarized supercurrents for spintronics: A review of current progress, *Rep. Prog. Phys.* **78**, 104501 (2015).
 - [7] J. Linder and A. V. Balatsky, Odd-frequency superconductivity, *Rev. Mod. Phys.* **91**, 045005 (2019).
 - [8] V. Krive, L. Y. Gorelik, R. I. Shekhter, and M. Jonson, Chiral symmetry breaking and the Josephson current in a ballistic superconductor-quantum wire-superconductor junction, *Low Temp. Phys.* **30**, 398 (2004).
 - [9] A. A. Reynoso, G. Usaj, C. A. Balseiro, D. Feinberg, and M. Avignon, Anomalous Josephson Current in Junctions with Spin Polarizing Quantum Point Contacts, *Phys. Rev. Lett.* **101**, 107001 (2008).
 - [10] A. Buzdin, Direct Coupling Between Magnetism and Superconducting Current in the Josephson ϕ_0 Junction, *Phys. Rev. Lett.* **101**, 107005 (2008).
 - [11] Y. Tanaka, T. Yokoyama, and N. Nagaosa, Manipulation of the Majorana Fermion, Andreev Reflection, and Josephson Current on Topological Insulators, *Phys. Rev. Lett.* **103**, 107002 (2009).
 - [12] A. Zazunov, R. Egger, T. Jonckheere, and T. Martin, Anomalous Josephson Current through a Spin-Orbit

- Coupled Quantum Dot, *Phys. Rev. Lett.* **103**, 147004 (2009).
- [13] A. G. Mal'shukov, S. Sadjina, and A. Brataas, Inverse spin Hall effect in superconductor/normal-metal/superconductor Josephson junctions, *Phys. Rev. B* **81**, 060502(R) (2010).
- [14] A. Brunetti, A. Zazunov, A. Kundu, and R. Egger, Anomalous Josephson current, incipient time-reversal symmetry breaking, and Majorana bound states in interacting multilevel dots, *Phys. Rev. B* **88**, 144515 (2013).
- [15] T. Yokoyama, M. Eto, and Y. V. Nazarov, Anomalous Josephson effect induced by spin-orbit interaction and Zeeman effect in semiconductor nanowires, *Phys. Rev. B* **89**, 195407 (2014).
- [16] F. S. Bergeret and I. V. Tokatly, Theory of diffusive φ_0 Josephson junctions in the presence of spin-orbit coupling, *Europhys. Lett.* **110**, 57005 (2015).
- [17] F. Konschelle, I. V. Tokatly, and F. S. Bergeret, Theory of the spin-galvanic effect and the anomalous phase shift φ_0 in superconductors and Josephson junctions with intrinsic spin-orbit coupling, *Phys. Rev. B* **92**, 125443 (2015).
- [18] G. Campagnano, P. Lucignano, D. Giuliano, and A. Tagliacozzo, Spin-orbit coupling and anomalous Josephson effect in nanowires, *J. Phys.: Condens. Matter* **27**, 205301 (2015).
- [19] D. Kuzmanovski, J. Linder, and A. Black-Schaffer, Quantum ground state control in superconductor-silicene structures: $0-\pi$ transitions, φ_0 -junctions, and Majorana bound states, *Phys. Rev. B* **94**, 180505(R) (2016).
- [20] M. Minutillo, D. Giuliano, P. Lucignano, A. Tagliacozzo, and G. Campagnano, Anomalous Josephson effect in S/SO/F/S heterostructures, *Phys. Rev. B* **98**, 144510 (2018).
- [21] W. Mayer, M. C. Dartiaillh, J. Yuan, K. S. Wickramasinghe, E. Rossi, and J. Shabani, Gate controlled anomalous phase shift in Al/InAs Josephson junctions, *Nat. Commun.* **11**, 212 (2020).
- [22] V. Braude and Yu. V. Nazarov, Fully Developed Triplet Proximity Effect, *Phys. Rev. Lett.* **98**, 077003 (2007).
- [23] R. Grein, M. Eschrig, G. Metalidis, and G. Schon, Spin-Dependent Cooper Pair Phase and Pure Spin Supercurrents in Strongly Polarized Ferromagnets, *Phys. Rev. Lett.* **102**, 227005 (2009).
- [24] J.-F. Liu and K. S. Chan, Anomalous Josephson current through a ferromagnetic trilayer junction, *Phys. Rev. B* **82**, 184533 (2010).
- [25] I. Kulagina and J. Linder, Spin supercurrent, magnetization dynamics, and φ -state in spin-textured Josephson junctions, *Phys. Rev. B* **90**, 054504 (2014).
- [26] A. Moor, A. F. Volkov, and K. B. Efetov, Chirality and spin transformation of triplet Cooper pairs upon interaction with singlet condensate, *Phys. Rev. B* **92**, 214510 (2015).
- [27] A. Moor, A. F. Volkov, and K. B. Efetov, Nematic versus ferromagnetic spin filtering of triplet Cooper pairs in superconducting spintronics, *Phys. Rev. B* **92**, 180506(R) (2015).
- [28] S. Mironov and A. Buzdin, Triplet proximity effect in superconducting heterostructures with a half-metallic layer, *Phys. Rev. B* **92**, 184506 (2015).
- [29] I. V. Bobkova, A. M. Bobkov, and M. A. Silaev, Gauge theory of the long-range proximity effect and spontaneous currents in superconducting heterostructures with strong ferromagnets, *Phys. Rev. B* **96**, 094506 (2017).
- [30] M. A. Silaev, I. V. Tokatly, and F. S. Bergeret, Anomalous current in diffusive ferromagnetic Josephson junctions, *Phys. Rev. B* **95**, 184508 (2017).
- [31] D. S. Rabinovich, I. V. Bobkova, A. M. Bobkov, and M. A. Silaev, Chirality selective spin interactions mediated by the moving superconducting condensate, *Phys. Rev. B* **98**, 184511 (2018).
- [32] S. Pal and C. Benjamin, Quantized Josephson phase battery, *Europhys. Lett.* **126**, 57002 (2019).
- [33] H. Meng, A. V. Samokhvalov, and A. I. Buzdin, Nonuniform superconductivity and Josephson effect in a conical ferromagnet, *Phys. Rev. B* **99**, 024503 (2019).
- [34] F. S. Bergeret, A. F. Volkov, and K. B. Efetov, Long-Range Proximity Effects in Superconductor-Ferromagnet Structures, *Phys. Rev. Lett.* **86**, 4096 (2001).
- [35] A. Kadigrobov, R. I. Shekhter, and M. Jonson, Quantum spin fluctuations as a source of long-range proximity effects in diffusive ferromagnet-superconductor structures, *Europhys. Lett.* **54**, 394 (2001).
- [36] M. Eschrig, J. Kopu, J. C. Cuevas, and G. Schön, Theory of Half-Metal/Superconductor Heterostructures, *Phys. Rev. Lett.* **90**, 137003 (2003).
- [37] M. Houzet and A. I. Buzdin, Long range triplet Josephson effect through a ferromagnetic trilayer, *Phys. Rev. B* **76**, 060504(R) (2007).
- [38] Y. Asano, Y. Tanaka, and A. A. Golubov, Josephson Effect due to Odd-Frequency Pairs in Diffusive Half Metals, *Phys. Rev. Lett.* **98**, 107002 (2007).
- [39] Y. Asano, Y. Sawa, Y. Tanaka, and A. A. Golubov, Odd-frequency pairs and Josephson current through a strong ferromagnet, *Phys. Rev. B* **76**, 224525 (2007).
- [40] M. Eschrig and T. Löfwander, Triplet supercurrents in clean and disordered half-metallic ferromagnets, *Nat. Phys.* **4**, 138 (2008).
- [41] A. V. Galaktionov, M. S. Kalenkov, and A. D. Zaikin, Josephson current and Andreev states in superconductor-half metal-superconductor heterostructures, *Phys. Rev. B* **77**, 094520 (2008).
- [42] M. S. Kalenkov, A. V. Galaktionov, and A. D. Zaikin, Josephson current in ballistic heterostructures with spin-active interfaces, *Phys. Rev. B* **79**, 014521 (2009).
- [43] A. F. Volkov and K. B. Efetov, Odd spin-triplet superconductivity in a multilayered superconductor-ferromagnet Josephson junction, *Phys. Rev. B* **81**, 144522 (2010).
- [44] L. Trifunovic and Z. Radović, Long-range spin-triplet proximity effect in Josephson junctions with multilayered ferromagnets, *Phys. Rev. B* **82**, 020505(R) (2010).
- [45] M. Alidoust and J. Linder, Spin-triplet supercurrent through inhomogeneous ferromagnetic trilayers, *Phys. Rev. B* **82**, 224504 (2010).
- [46] H. Meng, X. Wu, and Z. Zheng, Long-range triplet Josephson current modulated by the interface magnetization texture, *Europhys. Lett.* **104**, 37003 (2013).
- [47] R. S. Keizer, S. T. B. Goennenwein, T. M. Klapwijk, G. Miao, G. Xiao, and A. Gupta, A spin triplet supercurrent through the half-metallic ferromagnet CrO₂, *Nature (London)* **439**, 825 (2006).
- [48] I. Sosnin, H. Cho, V. T. Petrashov, and A. F. Volkov, Superconducting Phase Coherent Electron Transport in Proximity Conical Ferromagnets, *Phys. Rev. Lett.* **96**, 157002 (2006).

- [49] J. W. A. Robinson, J. D. S. Witt, and M. G. Blamire, Controlled injection of spin-triplet supercurrents into a strong ferromagnet, *Science* **329**, 59 (2010).
- [50] D. Sprungmann, K. Westerholt, H. Zabel, M. Weides, and H. Kohlstedt, Evidence for triplet superconductivity in Josephson junctions with barriers of the ferromagnetic Heusler alloy Cu_2MnAl , *Phys. Rev. B* **82**, 060505(R) (2010).
- [51] M. S. Anwar, F. Czeschka, M. Hesselberth, M. Porcu, and J. Aarts, Long-range supercurrents through half-metallic ferromagnetic CrO_2 , *Phys. Rev. B* **82**, 100501(R) (2010).
- [52] T. S. Khaire, M. A. Khasawneh, W. P. Pratt, Jr., and N. O. Birge, Observation of Spin-Triplet Superconductivity in Co-Based Josephson Junctions, *Phys. Rev. Lett.* **104**, 137002 (2010).
- [53] M. A. Khasawneh, T. S. Khaire, C. Klose, W. P. Pratt, Jr., and N. O. Birge, Spin-triplet supercurrent in Co-based Josephson junctions, *Supercond. Sci. Technol.* **24**, 024005 (2011).
- [54] C. Klose, T. S. Khaire, Y. Wang, W. P. Pratt, Jr., N. O. Birge, B. J. McMorran, T. P. Ginley, J. A. Borchers, B. J. Kirby, B. B. Maranville, and J. Unguris, Optimization of Spin-Triplet Supercurrent in Ferromagnetic Josephson Junctions, *Phys. Rev. Lett.* **108**, 127002 (2012).
- [55] W. M. Martinez, W. P. Pratt, Jr., and N. O. Birge, Amplitude Control of the Spin-Triplet Supercurrent in S/F/S Josephson Junctions, *Phys. Rev. Lett.* **116**, 077001 (2016).
- [56] J. A. Glick, S. Edwards, D. Korucu, V. Aguilar, B. M. Niedzielski, R. Loloee, W. P. Pratt, Jr., N. O. Birge, P. G. Kotula, and N. Missert, Spin-triplet supercurrent in Josephson junctions containing a synthetic antiferromagnet with perpendicular magnetic anisotropy, *Phys. Rev. B* **96**, 224515 (2017).
- [57] D. Massarotti, N. Banerjee, R. Caruso, G. Rotoli, M. G. Blamire, and F. Tafuri, Electrodynamics of Josephson junctions containing strong ferromagnets, *Phys. Rev. B* **98**, 144516 (2018).
- [58] B. M. Niedzielski, T. J. Bertus, J. A. Glick, R. Loloee, W. P. Pratt, Jr., and N. O. Birge, Spin-valve Josephson junctions for cryogenic memory, *Phys. Rev. B* **97**, 024517 (2018).
- [59] V. Aguilar, D. Korucu, J. A. Glick, R. Loloee, W. P. Pratt, Jr., and N. O. Birge, Spin-polarized triplet supercurrent in Josephson junctions with perpendicular ferromagnetic layers, *Phys. Rev. B* **102**, 024518 (2020).
- [60] D. Sanchez-Manzano, S. Mesoraca, F. A. Cuellar *et al.*, Extremely long-range, high-temperature Josephson coupling across a half-metallic ferromagnet, *Nat. Mater.* **21**, 188 (2022).
- [61] N. Banerjee, J. W. A. Robinson, and M. G. Blamire, Reversible control of spin-polarized supercurrents in ferromagnetic Josephson junctions, *Nat. Commun.* **5**, 4771 (2014).
- [62] J. A. Glick Jr., V. Aguilar, A. B. Gougam, B. M. Niedzielski, E. C. Gingrich, R. Loloee, W. P. Pratt, Jr., and N. O. Birge, Phase control in a spin-triplet SQUID, *Sci. Adv.* **4**, eaat9457 (2018).
- [63] M. Egilmez, J. W. A. Robinson, J. L. MacManus-Driscoll, L. Chen, H. Wang, and M. G. Blamire, Supercurrents in half-metallic ferromagnetic $\text{La}_{0.7}\text{Ca}_{0.3}\text{MnO}_3$, *Europhys. Lett.* **106**, 37003 (2014).
- [64] P. Quarterman, C. Sun, J. Garcia-Barriocanal, M. DC, Y. Lv, S. Manipatruni, D. E. Nikonov, I. A. Young, P. M. Voyles, and J. P. Wang, Demonstration of Ru as the 4th ferromagnetic element at room temperature, *Nat. Commun.* **9**, 2058 (2018).
- [65] P. G. de Gennes, *Superconductivity of Metals and Alloys* (Benjamin, New York, 1966), Chap. 5.
- [66] See Supplemental Material at <http://link.aps.org/supplemental/10.1103/PhysRevB.106.174502> for the introduction of experimental implementation and the dependence of the Josephson current on interface parameters.
- [67] G. Eilenberger, Transformation of Gorkov's equation for type II superconductors into transport-like equations, *Z. Phys.* **214**, 195 (1968).
- [68] K. D. Usadel, Generalized Diffusion Equation for Superconducting Alloys, *Phys. Rev. Lett.* **25**, 507 (1970).
- [69] C. R. Reeg and D. L. Maslov, Proximity-induced triplet superconductivity in Rashba materials, *Phys. Rev. B* **92**, 134512 (2015).
- [70] H. Meng, Y. Ren, J. E. Villegas, and A. I. Buzdin, Josephson current through a ferromagnetic bilayer: Beyond the quasiclassical approximation, *Phys. Rev. B* **100**, 224514 (2019).
- [71] C. Visani, Z. Sefrioui, J. Tornos, C. Leon, J. Briatico, M. Bibes, A. Barthélémy, J. Santamaría, and J. E. Villegas, Equalspin Andreev reflection and long-range coherent transport in high-temperature superconductor/half-metallic ferromagnet junctions, *Nat. Phys.* **8**, 539 (2012).
- [72] C. Visani, F. Cuellar, A. Pérez-Muñoz, Z. Sefrioui, C. León, J. Santamaría, and J. E. Villegas, Magnetic field influence on the proximity effect at $\text{YBa}_2\text{Cu}_3\text{O}_7/\text{La}_{2/3}\text{Ca}_{1/3}\text{MnO}_3$ superconductor/half-metal interfaces, *Phys. Rev. B* **92**, 014519 (2015).
- [73] Z. Radović, N. Lazarides, and N. Flytzanis, Josephson effect in double-barrier superconductor-ferromagnet junctions, *Phys. Rev. B* **68**, 014501 (2003).
- [74] K. Halterman and O. T. Valls, Layered ferromagnet-superconductor structures: The π state and proximity effects, *Phys. Rev. B* **69**, 014517 (2004).
- [75] Z. Pajović, M. Božović, Z. Radović, J. Cayssol, and A. Buzdin, Josephson coupling through ferromagnetic heterojunctions with noncollinear magnetizations, *Phys. Rev. B* **74**, 184509 (2006).
- [76] P. H. Barsic, O. T. Valls, and K. Halterman, Thermodynamics and phase diagrams of layered superconductor/ferromagnet nanostructures, *Phys. Rev. B* **75**, 104502 (2007).
- [77] K. Halterman, P. H. Barsic, and O. T. Valls, Odd Triplet Pairing in Clean Superconductor/Ferromagnet Heterostructures, *Phys. Rev. Lett.* **99**, 127002 (2007).
- [78] K. Halterman and O. T. Valls, Emergence of triplet correlations in superconductor/half-metallic nanojunctions with spin-active interfaces, *Phys. Rev. B* **80**, 104502 (2009).
- [79] K. Halterman, O. T. Valls, and C.-T. Wu, Charge and spin currents in ferromagnetic Josephson junctions, *Phys. Rev. B* **92**, 174516 (2015).
- [80] K. Halterman and M. Alidoust, Half-metallic superconducting triplet spin valve, *Phys. Rev. B* **94**, 064503 (2016).
- [81] K. Halterman and M. Alidoust, Josephson currents and spin-transfer torques in ballistic SFSFS nanojunctions, *Supercond. Sci. Technol.* **29**, 055007 (2016).
- [82] C.-T. Wu and K. Halterman, Spin transport in half-metallic ferromagnet-superconductor junctions, *Phys. Rev. B* **98**, 054518 (2018).
- [83] M. Alidoust and K. Halterman, Half-metallic superconducting triplet spin multivalves, *Phys. Rev. B* **97**, 064517 (2018).
- [84] K. Halterman and M. Alidoust, Induced energy gap in finite-sized superconductor/ferromagnet hybrids, *Phys. Rev. B* **98**, 134510 (2018).

- [85] K. Halterman, M. Alidoust, R. Smith, and S. Starr, Supercurrent diode effect, spin torques, and robust zero-energy peak in planar half-metallic trilayers, *Phys. Rev. B* **105**, 104508 (2022).
- [86] P. F. Bagwell, Suppression of the Josephson current through a narrow, mesoscopic, semiconductor channel by a single impurity, *Phys. Rev. B* **46**, 12573 (1992).
- [87] C. W. J. Beenakker, Universal Limit of Critical-Current Fluctuations in Mesoscopic Josephson Junctions, *Phys. Rev. Lett.* **67**, 3836 (1991).
- [88] J. Bardeen, R. Kümel, A. E. Jacobs, and L. Tewordt, Structure of vortex lines in pure superconductors, *Phys. Rev.* **187**, 556 (1969).
- [89] J. Cayssol and G. Montambaux, Exchange-induced ordinary reflection in a single-channel superconductor-ferromagnet-superconductor junction, *Phys. Rev. B* **70**, 224520 (2004).
- [90] L. N. Bulaevskii, A. I. Buzdin, M. L. Kulić, and S. V. Panyukov, Coexistence of superconductivity and magnetism theoretical predictions and experimental results, *Adv. Phys.* **34**, 175 (1985).